21st IAEA Fusion Energy Conference
Chengdu, China, 16 - 21 October, 2006

IAEA-CN-149/ OV/4-4

Experimental Progress on Zonal Flow Physics in Toroidal Plasmas

A. Fujisawa et al.

NIFS-835

Oct. 2006

Experimental Progress on Zonal Flow Physics in Toroidal Plasmas

A. Fujisawa, T. Ido, A. Shimizu, S. Okamura, K. Matsuoka, Y. Hamada, [1]K. Hoshino, [2]Y. Nagashima, [1]K. Shinohara, H. Nakano, S. Ohshima, [1]Y. Miura, K. Itoh, S. –I. Itoh, *NIFS,* [1]*JAERI,* [2]*RIAM, Japan*
[3]M. Shats, [3]H. Xia, [3]*ANU, Australia*
[4]J. Q. Dong, [5]T. Lan, [4]L. W. Yan, [4]K. J. Zhao, [4]*SWIP,* [5]*Univ. Sci. & Tech., China*
[6]G. D. Conway, [7]U. Stroth, [6]*Max-Planck institute,*[7]*Universität Stuttgart, Germany*
[8]A. Melnikov, [8]*Kurchatov Institute, Russia*
[9]C. Hidalgo, [9]*CIEMAT, Spain*
[10]G. R. Tynan, [11]G. R. Mckee, [10]C. Holland, [11]R. J. Fonck, [11]D. K. Gupta, [10]P. H. Diamond, [10]*UCSD,* [11]*Univ. Wisconsin U.S.A.*
Corresponding e-mail: fujisawa@nifs.ac.jp

Abstract

Present status of experiments on zonal flows is overviewed. Innovative use of traditional and modern diagnostics has revealed unambiguously the existence of zonal flows, their spatio-temporal characteristics, their relationship with turbulence, and their effects on confinement. Particularly, a number of observations have been accumulated on the oscillatory branch of zonal flows, dubbed geodesic acoustic modes, suggesting necessity of theories to give their proper description. In addition to these basic properties of zonal flows, several new methods have elucidated the zonal flow generation processes from turbulence. Further investigation of relationship between zonal flows and confinement is strongly encouraged as cross-device activity including low temperature toroidal and linear devices.

1. Introduction

Drift-wave turbulence has been extensively studied for a long time to clarify anomalous transport governing the toroidal plasma confinement [1,2]. The discovery of H-mode [3] highlighted the effect of macroscopic flow or radial electric field on the turbulence, and self-organization process of flow and turbulence. Recently, theories and simulations have argued the existence of another important player, *i.e.,* zonal flow – mesoscale structure of radial electric field [4,5]. In other words, the level of zonal flows controls the transport level, therefore, the performance of toroidal plasmas including ITER. Following the theoretical expectation, the existence of zonal flows has been experimentally confirmed, and the experiments on zonal flows have been made a great progress thanks to worldwide efforts in a number of toroidal devices. This paper aims at the integration of the distributed experimental results on zonal flows. The content includes the basic features of zonal flows in structure and dynamics, dependencies of zonal flow characteristics on plasma parameters and magnetic configurations, and the quantification of their impacts on the turbulence and transport.

2. Experimental Physics of Zonal Flows

Zonal flows are fluctuations linearly stable but nonlinearly driven by turbulence. The zonal flows are characterized by their symmetric nature around magnetic axis, that is, m=n=0 structure in poloidal and toroidal directions, and has rapidly varying structure with a finite wavelength in radial direction. The symmetric characteristics causes no cross-field transport associated with zonal flow. The experimental identification of zonal flows requires two major issues; to find fluctuating structure to satisfy m=n=0 and $k_r \neq 0$, and to confirm that the structure are generated by background turbulence.

Two kinds of zonal flows have been expected in toroidal plasmas; stationary zonal flows and geodesic acoustic modes (GAMs)[6]. Stationary zonal flows fluctuate in quite low frequency, while GAM is an oscillatory branch. The m=1 asymmetry of toroidal plasma is the driving force of GAM. The density fluctuation of m=1 is expected to be accompanied with GAM, while no significant density fluctuation is expected for stationary zonal flows. Theories expect that the GAM frequency should be expressed as $f_{GAM} \propto c_s/R$, where c_s and R represent the sound wave velocity and the major radius of the device, respectively.

In experiments, zonal flows can be detected by direct measurement of plasma flow or radial electric field. The Langmuir probes are the simplest method to detect zonal flows through electrostatic potential measurement [7,8], although the applicable region is limited to the plasma edge in the modern high temperature plasmas. The heavy ion beam probe (HIBP) is one to detect electrostatic potential inside high temperature core of plasmas [9-14]. Besides, the other methods to detect flow indirectly have been developed recently, such as beam emission spectroscopy (BES) with time-delay-estimation technique (TDE) [14] and Doppler reflectometry (DR) [15]. The experimental results related to zonal flows that have ever been obtained are summed up in table 1.

As is shown in table 1, the zonal flow experiments take place over a wide range of plasma parameters in a variety of devices in. In physical sense, dimensionless studies extensively performed in TJ-K contribute to systematic physical understanding of plasma turbulence by giving a bridge between plasmas in quite different range of parameters, *i.e.,* large fusion-oriented researches and university laboratories for fundamental plasma study [16].

3. Fundamental Observations on Zonal Flows

3-1 Fluctuation Spectra

A fundamental observation to study a system of zonal flow and drift wave turbulence is to obtain fluctuation spectrum. Figure 1 shows examples of frequency spectra in CHS, T-10, TEXT and JFT-2M (measured with HIBPs), together with those in ASDEX-U (measured with Doppler reflectometry) and from DIII-D (measured with BES). One common feature of the spectra in Fig. 1 is, obviously, the existence of solitary peaks, which are conjectured as GAMs. At present, many of fluctuation spectra measurements aiming at zonal flow identification have been performed in

frequency domain. Complementally, a few of wavenumber spectra have been obtained using Langmuir probe arrays in rather low temperature devices; CSDX [17], H1-heliac [18] and TJ-K [19].

Device	Diagnostics	Results [reference no.]
ASDEX-U R (m)/a(m)=1.65/0.5	**Doppler reflectometry** 50-75 GHz (O &X mode) estimated from Doppler shift frequency Observable range : r/a> ~0.7	- GAM frequency scaling; f_{GAM}~c_s/R - geometrical dependence of GAM frequency (q and k) is investigated - GAM localization at the plasma edge (~0.97) [15]
CASTOR R(m)/a(m)=0.4/0.085	**Langmuir probes**	- development of autocorrelation width technique to detect Stationary zonal flows [20]
CHS R (m) /a(m)=1.0/0.2	**HIBPs** (3ch./each) Observing at two different toroidal positions separated by 90. observable range: 0<r/a<1	- identification of stationary zonal flows [10] - turbulence is modulation with stationary zonal flows [41] - energy transfer between turbulence and zonal flows [40] - eigenmode characteristics of GAM [27]
CLD L(m)/a(m)=1.6/0.03	**Langmuir probes**	- development of method to detect stationary zonal flow [21]
CSDX **(linear machine)** L/a(m)=3./0.045	**Langmuir probes**	- wavenumber spectrum in fully developed turbulence [34] - Reynolds stress estimation for flow drive [17]
DIII-D R (m)/a(m)=1.7/0.6	**Beam Emission Spectroscopy** 2-D array (16 channels) with TDE technique observable range: 0.65<r/a<1, **Langmuir probe** at plasma edge and SOL	- GAM frequency scaling; f_{GAM}~c_s/R [14]. - q-dependence of GAM frequency [25]. - bicoherence analysis before and after H-mode transition [33]
H1 R (m) /a(m)=1.0/0.2	**Triple probe arrays** radially and poloidally aligned	-identification of GAM [7] - energy transfer between disparate scale fluctuation [18,39] - randomization effects of zonal flows on turbulence [42] - behavior of GAM before and after LH-transition [26]
HL-2A R(m)/a(m)=1.65/0.4	**Three step Langmuir probe arrays**	-systematic identification of GAM [23]; m=n=0
HT-6M R(m)/a(m)=0.65/0.19	**Tripe and Mach probes**	- Reynolds stress measurement during H-mode transition [30]
HT-7 R(m)/a(m)=1.22/0.27	**Forked Langmuir probe**	- identification of stationary zonal flow [8]
JFT-2M R (m) /a(m)=1.3/0.3	**HIBP** (6-7 ch.) observable range: 0.8 <r/a<1 **Reciprocating Langmuir Probes** at the plasma edge	- eigenmod and propagation e characteristics of GAM [12] - turbulence modulation with GAM. [24] - symmetric property of GAM; m~0 (<1.5) [12,24] - bicoherence analysis for coupling between GAM and turbulence [22,35]
JIPPT-IIU R(m)/a(m)=0.93/0.23	**HIBP** (6-7 ch.) observable range : 0.2<r/a<1	- fundamental study of GAM; m~0 is confirmed for GAM [11] - streamer study [43]
T-10 R (m) /a(m)=1.5/0.3	**HIBP** (3ch.) observable range: 0.57 <r/a<1 **Correlation reflectometor**	- symmetric property of GAM; m~0. - frequency scaling of GAM; f_{GAM}~c_s/R - spatial property of GAM; relation with the rational surfaces, - Intermittent nature of GAM & density threshold [13]
TEXT-U R (m) /a(m)=1.0/0.27	**HIBP** (3 ch) observable range: 0<r/a<1	- GAM in potential fluctuation [9]
TJ-II R (m) /a(m)=1.5/0.22	**Langmuir Probe s**	- Reynolds stress measurement at the plasma edge [29]
TJ-K R (m) /a(m)=0.6/0.1	**Probe arrays**	- dimensionless analysis of turbulence [16,19]

Table 1: The present status of experiments on zonal flows.

Correlation property of fluctuation in the observable frequency range has been measured with twin HIBPs in CHS. The fluctuation spectrum can be divided roughly into three characteristic frequency regions; I) stationary zonal flow region in low frequency regime (less than ~1 kHz in CHS) to show a long-distance correlation, II) sharp peaks conjectured as GAMs to show a long-

distance correlation, and III) broad-band turbulence (around 50 kHz in CHS) with short correlation length. This classification could be applied on the spectra of the other toroidal devices.

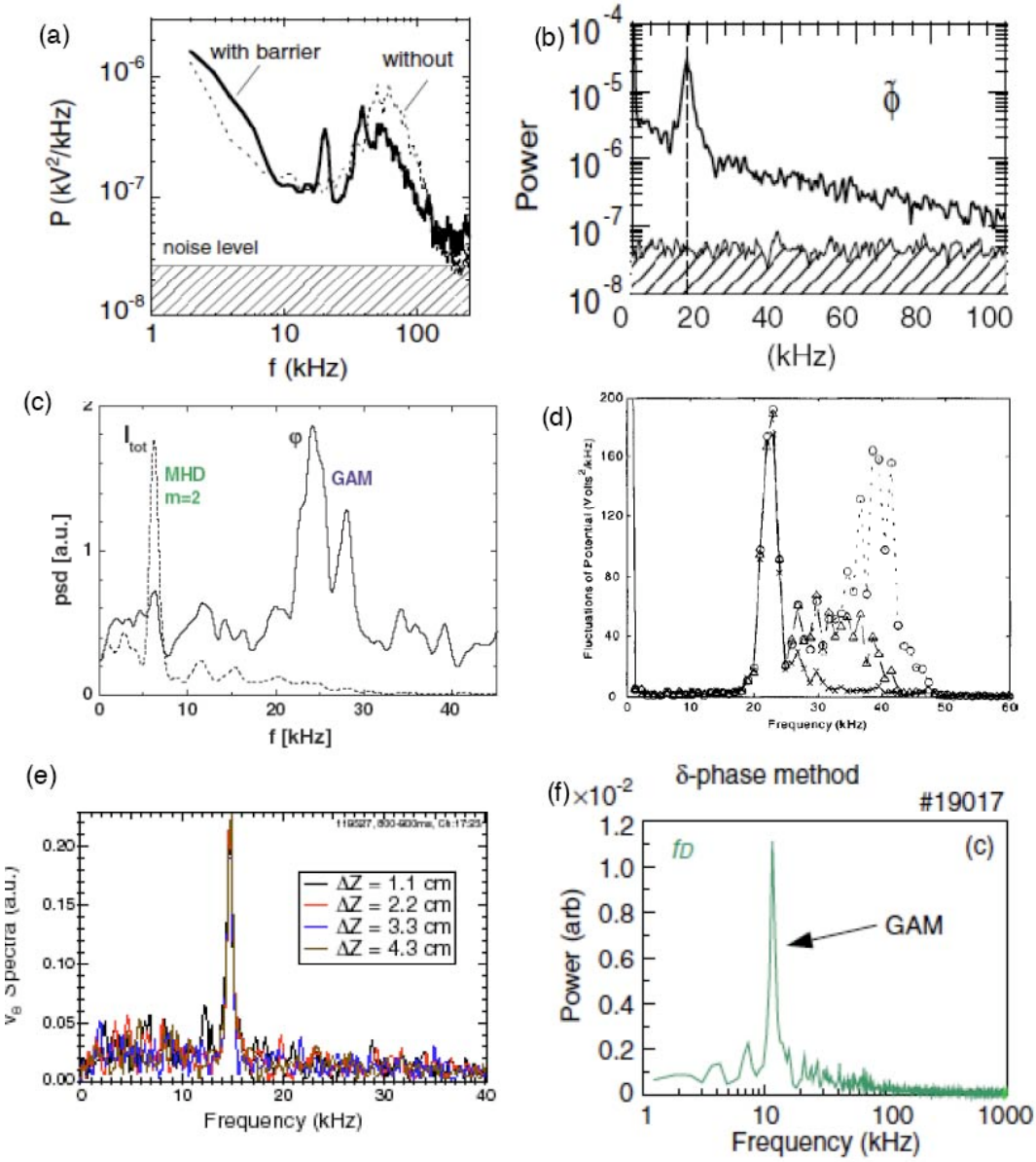

Figure 1. Potential Fluctuation spectra measured with HIBP. (a) Electric field fluctuation in CHS [41]. (b) Potential fluctuation spectra in JFT-2M [12] (c)T10 [13] (d) TEXT -U [9] (e) Velocity fluctuation spectra measured with BES in DIII-D [14]. (f) Spectrum of Doppler frequency measured with Doppler reflectometry in ASDEX-U [15].

3-2. Stationary Zonal Flows

Identification of stationary zonal flow essentially needs multipoint detection of flow or radial electric field in order to prove its symmetric nature. Several methods without multipoint detection have been also invented to detect stationary zonal flows; for example, autocorrelation width technique applied

in CASTOR tokamak [20] and detection technique of Doppler frequency modulation due to zonal flow in Colombia Linear Machine (CLM) [21]. A pioneering work to search the stationary zonal flows was performed in HT-7 tokamak using a forked Langmuir probe, reporting the existence of long-poloidal wavelength EXB time varying flow to satisfy the requirement of zonal flows [8].

Identification of zonal flows in high temperature core succeeded in CHS using twin HIBPs located at two different toroidal positions apart by 90 degree [10]. The measurement system confirms that the electric field fluctuation ranging from ~0.5 to ~1kHz should have toroidal symmetry of n=0 with finite radial wave numbers. Figure 2 shows radial correlation function between electric field at r=12 cm and the other location varying from 10 cm to 14cm, showing the spatio-temporal pattern of the stationary zonal flows. The observation shows the zonal flows with a finite radial wavelength of ~1 cm do exist, and the zonal flow loses the memory of structure in ~2 ms.

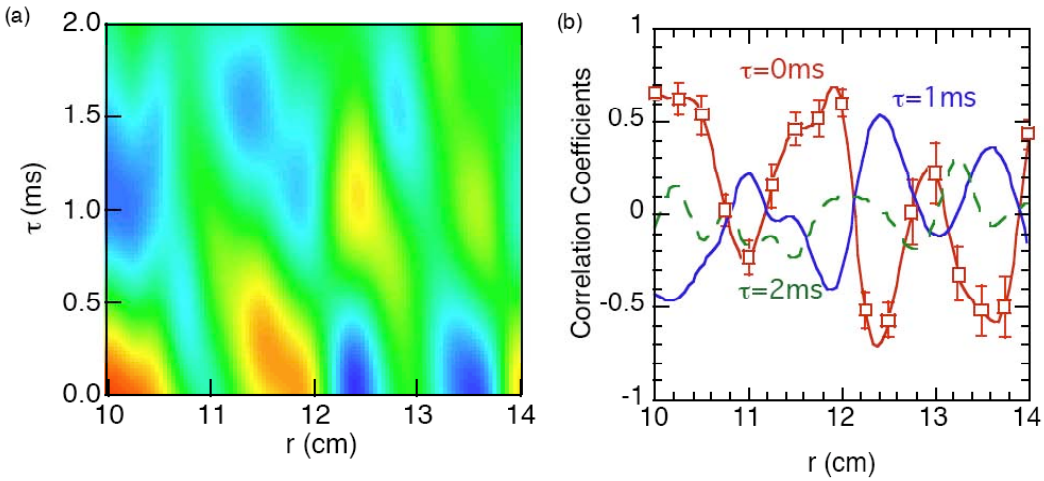

Figure 2. (a) Spatio-temporal structure of stationary zonal flows evaluated from correlation function. (b) Spatial correlation with the time lag of τ=0 ms, 1ms and 2ms.

3-3. GAMs

It could be easier to capture a signature of GAMs than the stationary zonal flows owing to its oscillatory nature. Following the GAM identification in H1-heliac [7], solitary peaks have been found in fluctuation spectra of a number of toroidal plasmas (see Fig. 1). The multi-channel property of HIBP is used to obtain the poloidal mode number of the oscillation. In JIPPT-IIU [11], JFT-2M [12] and T-10 [13], the poloidal mode numbers of the oscillations are inferred as m~0, proving that the mode should be GAMs (see table 1). In DIII-D, the multipoint detection also proves that the observed solitary mode should have m=0 poloidal mode structure [14]. The other multi-channel array Langmuir probes in H1 [7] and JFT-2M [22] also show the poloidal symmetric structure of the mode (m=0). Recently, in the Chinese device, HL-2A, the complete symmetric characteristics of m=n=0 have been confirmed using probe measurements in the edge of Ohmic discharges [23].

The variability of observation points of diagnostics can estimate the radial localization or

extent of the modes in JFT-2M (HIBP), T-10 (HIBP), CHS (HIBP), DIII-D (BES) and ASDEX-U (DR). Commonly, the modes (GAMs) are found to localize in rather narrow radial extent of a few cm for these cases. The observation in JFT-2M reported the eigenmode characteristics of the GAM, that is, the mode is localized in ~5 cm inside the separatrix without a change of frequency, while the electron temperature increases significantly toward core (see Fig. 3). In addition, the outward propagation characteristics of the GAM are induced, as is shown in Fig. 3 [24].

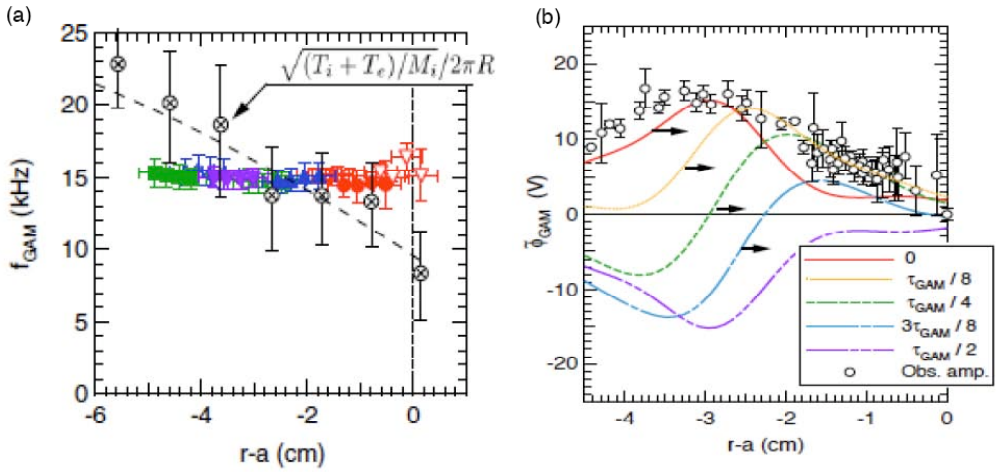

Figure 3. GAM structure in JFT2M. (a) GAM frequency as a function of radius. (b) The temporal change of GAM structure that indicates outward propagation.

The experimental GAM frequency has been compared with the theoretical expectation in a number of devices. In every trial, it is confirmed that the GAM frequency should be proportional to the sound velocity although somewhat different coefficient is found in different conditions even in the same devices. In ASDEX-U, the frequency dependence on the geometrical factors is investigated, such as safety factor q and ellipticity κ. The results suggest strong inverse and weak non-inverse dependences on k and q, respectively [15]. Figure 4 shows the observed GAM frequencies in different devices as a function of c_s/R.

In DIII-D, the dependence of GAM amplitude on q was investigated [25]. It is found that the GAM amplitude tends to increase as q-value increases, while opposite tendency was found in a situation. The positive dependence of the GAM amplitude on q-value suggests that the process of Landau damping should be important to determine the GAM level. In comparison, the amplitudes of GAM are much stronger in tokamaks than in helicals (CHS and H1). The analysis in H1-heliac indicates that the larger inhomogeneity of magnetic field configuration of helical plasma is the cause of the small fraction of zonal flow component [26]

It is found in an ECR-heated plasma of CHS that two different modes conjectured as GAMs coexist in a quite narrow range of frequency (actually at 16 kHz and 18kHz). The two modes show quite different radial distributions, and the features indicate eigenmode characteristics [27]. The

observation suggests that the GAM should have discrete frequencies, of which dependence obeys the theoretical expectation. In addition, the solitary peak is sharp but has a finite width to indicate finite lifetimes of GAMs. In fact, intermittent characteristics of GAMs have been reported in many devices; CHS, JFT-2M and T-10. In order to investigate spatial structure of GAM and temperature dependence of GAM frequency, the suggested eigenmode characteristics and intermittent nature should be taken into account for future analysis. A theory of GAM to consider the spatial dependency or localization is necessary to be built for comparison with experimental data.

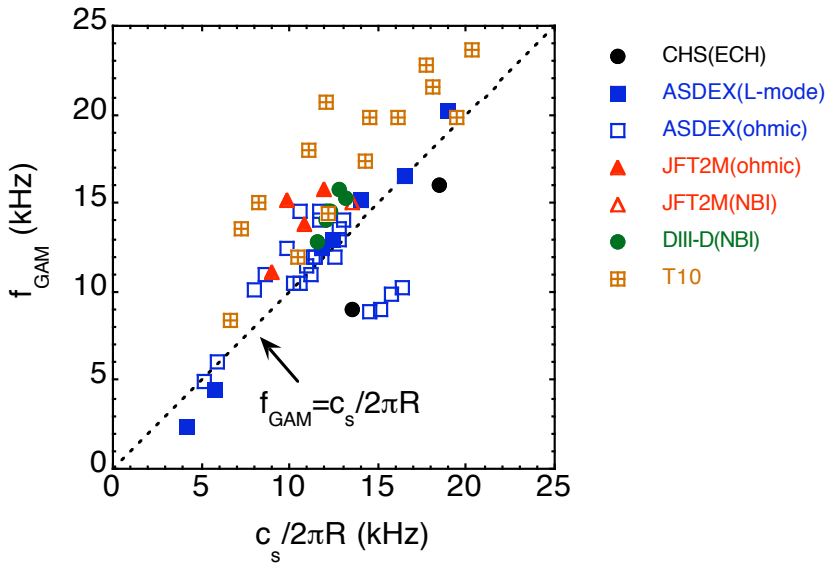

Figure 4. A comparison between observed GAM frequency and theoretical prediction. Here, c_s and R are the ion sound velocity and the major radius, respectively.

4. Nonlinear Interaction between Zonal Flows and Turbulence

4-1. Quantification of Flow Generation Process by Turbulence

It is considered that the zonal flows should be generated by turbulence through three-wave couplings expressed by the $\langle v\partial v\rangle$ nonlinearity(or the Reynolds stress term), similarly to the mean flow. The Reynolds stress has been directly evaluated in the edge regions of high temperature plasmas [28,29] and low temperature plasma such as CDSX [16]. Particularly, the Reynolds stress measurements at the edge of HT-6M suggested that the mean flow in the H-mode transition should be generated by turbulence [30], consistently with Prey & Predator model [31].

The strength of three-wave couplings can be qualified with bicoherence analysis [32]. The definition of the bicoherence is $b_c=|\langle g_{f3}^{*}g_{f2}g_{f1}\rangle|^2 /(\langle |g_{f3}|^2\rangle\langle|g_{f2}\ g_{f1}|^2\rangle)$, where g_f being the Fourier coefficient at a frequency f_3, and $f_1+f_2=f_3$ is satisfied, and $\langle\rangle$ represents the ensemble average. Therefore, the bicoherence can measure phase-coherency between different frequency waves, and the bicoherence value becomes large if phase coherency between three waves f_1, f_2, and f_3 is high. An increase in bicoherence was found in the transient phase from L to H-mode, which implies that an

increase in Reynolds stress is the cause to generate the large mean flow in H-mode [33].

The bicoherence analysis has been applied to prove the existence of couplings between turbulent waves in CSDX [34], H1-Heliac [7], HL-2 [23], HT-7 [8], and JFT-2M [35]. For example, the bicoherence diagrams in JFT-2M are shown in Fig. 5. In JFT-2M, the bicoherence analysis was applied on the potential fluctuation measured with Langmuir probe at the plasma edge. The diagrams show, obviously, the lines of $f_1+f_2=\pm 10$ kHz shows a clear high level of coupling, and the biphase is constant on the lines. Therefore, the bicoherence clearly demonstrates the existence of the coupling between GAM and turbulence, and that the modulational instabilities should be associated with the zonal flow generation [4]. A theoretical base is proposed to connect the obtained bicoherence value to the strength of three wave couplings [36].

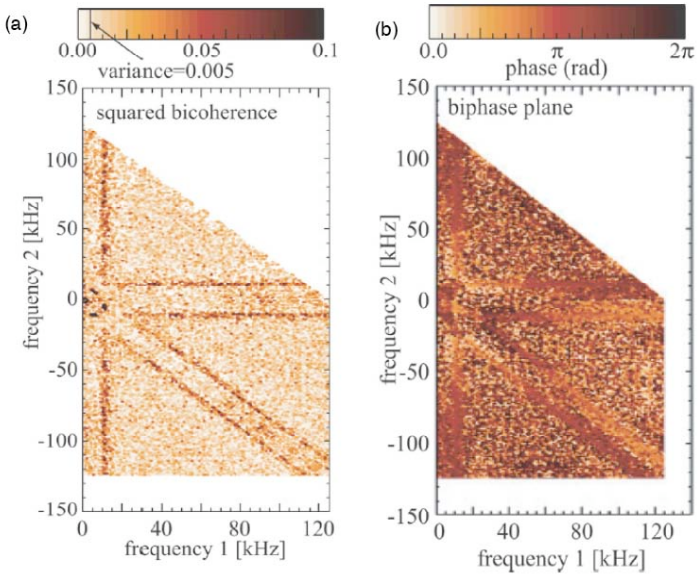

Figure 5. Bicoherence analysis to show coupling between GAM and background turbulence in JFT-2M. (a) Bicoherence evaluated with potential fluctuation at the plasma edge, and (b) corresponding biphase.

4-2. Energy Transfer between Zonal Flows and Turbulence

Energy transfer between disparate scale waves or fluctuations has been studied using nonlinear energy transfer [37] and autocorrelation analyses [38] in H1-heliac. These analyses have shown the evidence of inverse cascade in both frequency and wavenumber domains, and difference of energy transfer structure between L- and H-mode [17,26,39]. In a linear machine, CSDX, the fluctuation with low poloidal wavenumber, which is linearly stable, is found to develop as turbulence state is realized with an increase in magnetic field [16,34]. This suggests that the turbulence energy is transferred nonlinearly from turbulence into zonal flows in the wave-number domain.

The wavelet analysis reveals the temporal correlation between disparate-scale components of electric field fluctuation [40]. Figure 6 demonstrates the temporal evolutions of wavelet powers of

these three fluctuation regimes. It is obvious that the lower frequency regime close to stationary zonal flow (2.5<f<10kHz, called here zonal flows' tail) is anti-correlated with the power of turbulence (30<f<250 kHz). On the other hand, the power of GAM shows no significant correlation with those of tail and turbulence. Note that here the powers are normalized by total power in order to remove the variation of total fluctuation power, which may be associated with a change in bulk plasma parameters such as a pressure gradient. A recent study suggests that both powers of tail and turbulence are modulated by the zonal flow phase. Further investigation is necessary to elucidate the energy transfer between the fluctuation components; stationary zonal flow, tail, GAM and turbulence.

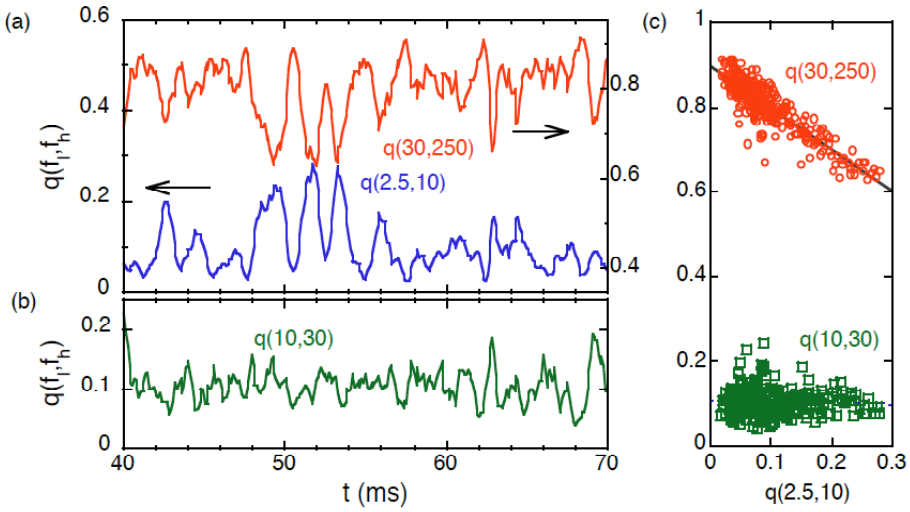

Figure 6. Wavelet power relationship between turbulence, GAM and tail fluctuation in CHS. (a) The power of tail shows anti-correlated with that of turbulence in time evolution. (b) Powers of turbulence and GAM as a function of that of zonal flow tail.

4-3. Role of Zonal Flows on Transport and Confinement

So far we have had a few experiments to demonstrate the effect of zonal flows on plasma transport and confinement. The HIBPs is able to estimate particle transport through simultaneous detection of density and potential fluctuations. It is found utilizing the advantage that the particle transport should be modulated with the zonal flow phase in CHS. Figure 7 shows the modulation effect of stationary zonal flow on turbulence. Here, instantaneous fluctuation amplitudes of density and potential are evaluated using the Gabour's wavelet transformation, and fluctuation-driven particle flux was calculated [41]. In addition, a significant change in potential fluctuation spectrum is deduced by taking a conditional average according to the zonal flow phases; maxima, minima and zero phases. Figure 7b demonstrates clear difference of fluctuation spectrum according to the zonal flow phase. However, one should be cautious on the fact that the measured potential fluctuation could contain electric field fluctuations along the probing beam orbit.

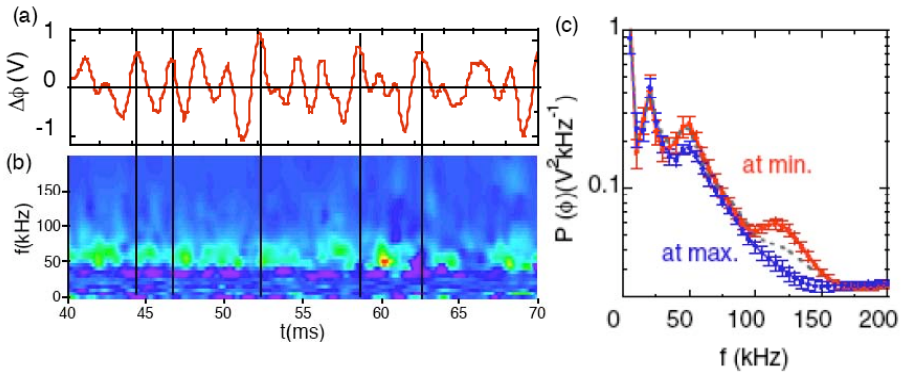

Figure 7. The modulation effect of stationary zonal flow on particle transport. (a) Temporal evolutions of stationary zonal flows and (b) an image plot of particle flux. (c) Conditional averages of potential fluctuation spectra in the time windows discriminated by the phase of zonal flow; i.e. maxima, zero and minima.

Similar analysis was performed in JFT-2M to study the relation between the GAM and turbulence [12,24]. Figure 8 shows the temporal evolutions of the band-pass filtered potential at GAM frequency and wavelet spectrum of density fluctuation. The density fluctuation appears to be modulated by the GAM frequency. Figure 8b shows the Fourier spectrum on evolution of the wavelet power of density fluctuation ranging from 100 kHz to 120 kHz. Obviously, the Fourier spectrum indicates a sharp peak consistent with GAM frequency. As a result, it is confirmed that the density fluctuation is modulated with the GAM evolution.

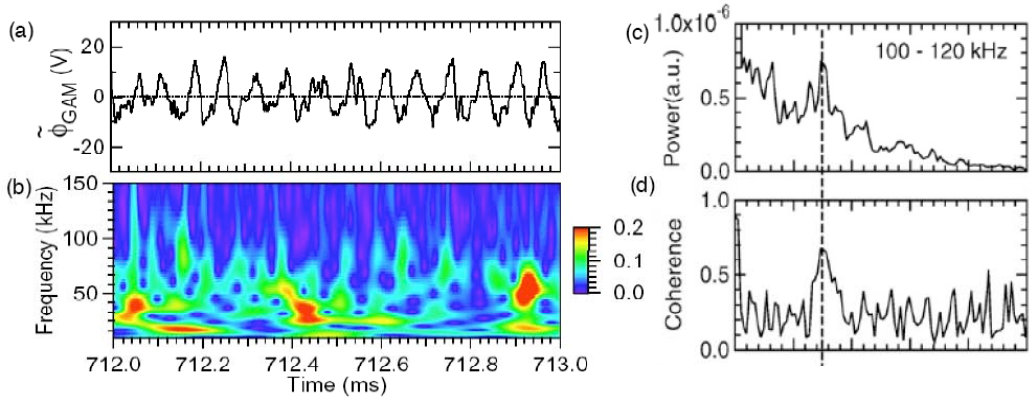

Figure 8. The modulation effect on turbulence. (a) Time evolution of potential at GAM frequency, and (b) that of the normalized density fluctuation. (c) Power spectrum of the density fluctuation amplitude whose frequency ranges from 100 to 120 kHz, and (b) its coherence with GAM fluctuation.

Several ways for the zonal flows to affect turbulence and resultant transport are expected, such as time-dependent electric field shearing, energy transfer between them, and so on. It is found in

H1-heliac that the phase randomization of fluctuations due to zonal flow should be the major cause to reduce the turbulence driven transport [42]. Although the present experimental precision in high temperature core cannot tell what mechanism is dominant for the turbulence regulation in the high temperature plasmas, the observations show the existence of significant coupling between zonal flow and turbulence.

5. Discussion and Summary

The presented experimental results have confirmed using many diagnostics techniques that the zonal flows really do exist in toroidal plasmas. The observations of the zonal flows have been accumulated about spatio-temporal structures, couplings between zonal flows and turbulence, and effects of zonal flows on plasma confinement. Particularly, many observations on basic features of GAMs have come from the world-wide devices. The important findings on GAMs are as follows; the GAMs are found localized in a rather narrow region of plasmas with a constant frequency, showing an eigen-mode property. The observed GAM frequency obeys the theoretical expectation. However, no theories are available to expect how the eigenmode having the observed frequency selectively grows in the real experimental situation.

A number of analysis techniques, such as bicoherence, have been applied to successfully prove the coupling between turbulence and zonal flows. Importantly, the experimental observations up to date have already demonstrated that the zonal flows really do regulate the plasma turbulence and resultant transports. Therefore, this experimental fact supports theoretical expectation that better confinement is achieved when the ratio of zonal flow to turbulence is larger, and indicates a future experimental direction to investigate what conditions the zonal flow can grow with suppressing turbulence. This answer is a key to optimize the magnetic configuration for confinement. Comparative works should be required amongst a wide variety of magnetic configurations and conditions to obtain the answer. Hence, the world-wide cooperation should be necessary to clarify the zonal flow physics and better confinement.

References

[1] P. C. Liewer, Nucl. Fusion **25** 543 (1985).

[2] A. Wootton et al Phys. Fluids B **2** 2879 (1990)

[3] F. Wagner et al., Phys. Rev. Lett.

[4] P. H. Diamond, K. Itoh, S. -I. Itoh, T. S. Hahm, Plasma Phys. Control. Fusion **47** R35 (2005)**.**

[5] Rosenbluth and Hinton, Phys. Rev. Lett.

[6] N. Winsor, J. L. Johnson, J. M. Dawson, Phys. Fluids **11** 2448 (1968).

[7] M. G. Shats et al., Phys. Rev. Lett. **90** 125002 (2003).

[8] G. S. Xu, B. N. Wan, M. Song, J. Li, Phys. Rev. Lett. **91** 125001 (2003).

[9] P. M. Schoch et al., Rev. Sci. Instrum. **74** 1846 (2003).
[10] A. Fujisawa et al., Phys. Rev. Lett. **93** 165002 (2004).
[11] Y. Hamada *et al* , Nucl. Fusion **45** 81 (2005).
[12] T. Ido et al., Nucl. Fusion **46** 512 (2006).
[13] A. V. Melnikov et al., Plasma Phys. Control. Fusion **48** 87 (2006)
[14] G. R. Mckee et al., Plasma Phys. Control. Fusion **45** A477 (2003).
[15] G. D. Conway et al., Plasma Phys. Control. Fusion **47** 1165 (2005).
[16] C. Lechte, S. Neidner, U. Stroth, New J. Phys. **4** 34 (2002).
[17] G. R. Tynan et al., Plasma Phys. Control. Fusion **48** S51 (2006).
[18] M. G. Shats, H. Xia, H. Punzmann, Phys. Rev. E **71** 046409 (2005).
[19] U. Stroth et al., Phys. Plasmas **11**, 2558 (2004).
[20] A. Bencze et al., Plasma Phys. Control. Fusion **48** S137 (2006).
[21] V. Sokolov, X. Wei, A. K. Sen, K. Avinash, Plasma Phys. Control. Fusion **48** S111 (2006).
[22]Y. Nagashima et al., Plasma Phys. Control. Fusion **48** S1(2006)
[23] K. J. Zhao, T. Lan, J. Q. Dong et al., Phys. Rev. Lett. **96** 255004 (2006).
[24] T. Ido et al., Plasma Phys. Control. Fusion **48** S41 (2006).
[25] G. R. McKee et al., Plasma Phys. Control. Fusion **48** S123 (2006).
[26] M. G. Shats, H. Xia, M. Yokoyama, Plasma Phys. Control. Fusion **48** S17 (2006).
[27] A. Fujisawa et al., Plasma Phys. Control. Fusion **48** S31 (2006).
[28] C. Hidalgo et al., Phys. Rev. Lett. **83** 2203 (1999).
[29] C. Hidalgo et al., Plasma Phys. Control. Fusion **48** S169 (2006).
[30] Y. H. Xu et al., Phys. Rev. Lett. **84** 3867 (2000).
[31] P. H. Diamond et al. Phys. Rev. Lett. **72** 2565 (1994).
[32] Y. C. Kim, E. J. Powers, IEEE Trans. Plasma. Sci. **PS-7** 120 (1979).
[33] G. R. Tynan, R. A. Moyer, M. J. Burin, C. Holland, Phys. Plasmas **8** 2691 (2001)
[34] M. J. Burin et al., Phys. Plasmas **12** 052320 (2005).
[35] Y. Nagashima et al., Phys. Rev. Lett. **95** 095002 (2005).
[36] K. Itoh et al., Phys. Plasmas **12** 102301 (2005).
[37] Ch. P. Ritz, E. J. Powers, R. D. Bengston, Phys. Fluids **B 1** 153 (1989).
[38]F. J. Crossley et al., Plasma Phys. Control. Fusion **34** 235 (1992).
[39] H. Xia and M. G. Shats, Phys. Rev. Lett **91** 155001 (2003).
[40] A. Fujisawa et al. Plasma Phys. Control. Fusion **48** A365 (2006).
[41] A. Fujisawa et al., Plasma Phys. Control. Fusion **48** S205 (2006).
[42] M. Shats, W. M. Solomon, H. Xia, Phys. Rev. Lett. **90** 125002 (2003).
[43] Y. Hamada et al., Phys. Rev. Lett. **96** 115003 (2006).